CrystEngComm

Accepted Manuscript

This article can be cited before page numbers have been issued, to do this please use: A. Gavezzotti, L. Lo Presti and S. Rizzato, *CrystEngComm*, 2022, DOI: 10.1039/D1CE01360B.

ROYAL SOCIETY OF CHEMISTRY

rsc.li/crystengcomm

View Article Online
DOI: 10.1039/D1CE01360B

HIGLIGHT

Molecular Dynamics simulation of organic materials: Structure, potentials and the MiCMoS computer platform

Received 00th January 20xx,
Accepted 00th January 20xx

DOI: 10.1039/x0xx00000x

Angelo Gavezzotti,*[a] Leonardo Lo Presti [b,c] and Silvia Rizzato [b,c]

The science of organic crystals and materials has seen in a few decades a spectacular improvement from months to minutes for an X-ray structure determination and from single-point lattice energy calculations to dynamic simulation of hundreds of thousands of atoms. While diffraction experiments now proceed in compact, almost tabletop apparatus, theoretical chemistry performs in comprehensive computer program environments that encode each particular way of modeling solid-state physics. Extremely fast experimental and theoretical advances expand the limits of what was thought possible just a few years ago, in search of new useful materials while shedding light on their complex nanoscale properties to an unprecedented degree of accuracy. In materials science theory the undisputed leader is Molecular Dynamics simulation, that provides a detailed picture of molecular events at atomic length and timescales. This Highlight traces a bit of history, clarifies a few fundamental points, and then illustrates the capabilities of a Molecular Simulation platform recently developed at the Chemistry Department of the Università degli Studi di Milano (Unimi), with high performance intermolecular potentials and case studies of large amplitude rotational diffusion, of the stability of crystalline clusters, and of anisotropic treatment of mechanical properties.

Introduction

The importance of a firm knowledge of molecular and crystal structure of organic compounds in solid-state theory can hardly be overemphasized and hardly needs an introduction. Applications range from materials science in general to drug formulation, pigments, energetic materials, organic semiconductors, to name a few. On the other hand, the best introduction to the experimental determination by X-ray diffraction of the bulk structure and properties of materials consisting of organic compounds is provided by Figure 1. In the first decades of the 20th century solving the crystal structure of a medium size organic molecule was something that might take the best part of one year with 50% success. The advent of the first computers in the 1960's caused a first dramatic drop to months of needed time, the second being when direct methods came on the scene with structures coming out in weeks. From then on, the downward slope became steeper and steeper with giant steps in instrumentation and computing. Presently, the full three-dimensional crystal structure of a 50-atom molecule comes out in a matter of minutes – faster than an NMR spectrum – out of a machine

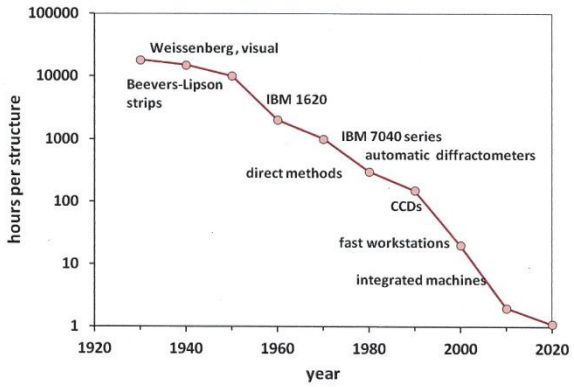

Figure 1. A sketch of the evolution of resources for the determination of solid-state structures for organic compounds.

whose size can be comparable to that of an IR spectrometer. Powder samples are handled almost as well, eliminating the bottleneck of single crystal availability.

Thanks to recent technical advances of great relevance, like for instance the development of lower emittance storage rings and of short wavelength, free-electron lasers,[1] fourth generation sources of synchrotron light now provide a wealth of information that goes far beyond classical X-ray crystallography. These include the study of femtosecond events,[2] of complex solid-state dynamics,[3] *in-situ* and *in-operando* phenomena,[4] and analyses of the structure of non periodic molecular clusters.[5] Protein structure may not even require diffraction anymore, if reconstruction by Cryo-EM (low-temperature electron microscopy)[6] holds its promises, as seems the case. In this context, computational techniques are likely to

[a] *Professor of Physical Chemistry (retired), Università degli Studi di Milano. E-mail: angelo.gavezzotti@unimi.it*
[b] *Department of Chemistry, Università degli Studi di Milano, Via Golgi 19, 20133 Milano, Italy.*
[c] *Istituto Nazionale di Fisica Nucleare (INFN), Laboratori Nazionali di Frascati, 00044 Frascati, Italy*

Electronic Supplementary Information (ESI) available: flowcharts of the organization of the MiCMoS platform (docx file).

become increasingly important. Computer simulation of equilibrium and non-equilibrium phenomena paves the way to the understanding of complexity at molecular scale, providing tools to interpret experimental outcomes within current theoretical frameworks.

The primary destination of the enormous amount of information streaming out of diffraction experiments is the Cambridge Structural Database (CSD)[7] now sporting its millionth entry. When incomplete, redundant, inaccurate, or plainly wrong material is (sometimes painstakingly) screened out, the CSD contains flawless structural information for about 150,000 organic crystals,[8] "organic" being compounds of carbon, hydrogen and the top rightmost part of the Periodic Table. Accurate hydrogen atom positions, crucial for computer simulation, are only in a few hundred reliable neutron diffraction studies; for the rest one has to make do with positions recomputed from approximate locations. This enormous amount of information is exploited by partial sampling for special issues, or by statistical techniques, some of which are still "old generation", like down-to-earth averaging or Principal Component Analysis. More sophisticated statistics has the new denomination of Artificial Intelligence, AI, sometimes providing new insight, and sometimes just rehashing old hat into a new buzzword. The CSD has been used in our laboratories over the years for statistical studies.[9–13]

The CSD only collects geometric information in the form of crystal cell dimensions, space group symmetry and atomic coordinates. Information on thermal parameters is not always accessible, especially for older structures. Nor there are data pertaining to materials like optical or mechanical properties, and even deposition of crystal shape and color, of crystallization conditions, or just of melting temperature, is only sporadic. It is up to a smart operator to derive explicit physical or energetic properties by downstream treatment of what is implicit in just atomic positions. In doing that, the obvious first step is the derivation of intermolecular potentials and forces, in a chemical perspective where the molecule and its structure play the key role and serve as support for the framework of potential energy schemes. This task that has been carried out repeatedly in our groups over the years[14–17] by merging geometry and thermodynamics.[18] The result are semiempirical but accurate formulations that afford lattice energies (potentials), mechanical properties (forces), and lattice dynamics (potentials and forces). Anything in the electromagnetic domain, like band structures and optoelectronic properties, of course require quantum chemical treatment.[19,20]

Parallel and complementary to the evolution of structure determination techniques has been the evolution of computing, not only in terms of sheer power (from kilo-flops to peta-flops) but in terms of levels of theory, from Hückel-type treatments in the 1950's to full inclusion of electron correlation in Molecular Orbital (MO) approaches, and with the derivation of accurate functionals and dispersion energy corrections[21] in Density Functional Theory (DFT). Collateral but vital turning points have been the introduction of Monte Carlo (MC)[22] and Molecular Dynamics (MD) methods, the latter split into a quantistic approach[23] and a classical mechanics approach.[24]

With the improvement of the joint powers of theory and of computer chips, any respectable and original theoretical chemistry group need have its own "platform", that is a set of software modules that can carry out the computations for the deployment of the theory. Whereas Schrödinger and Dirac conceived wave mechanics and spin without knowing what a computer is, in modern times no new idea in theoretical chemistry could sail without the support of a computer code; what is more, no theory or idea can be consecrated without independent check by a redistributed and well documented code. A good part of this Highlight is devoted to an illustration of the capabilities of the Milano Chemistry Molecular Simulation (MiCMoS) platform:
https://sites.unimi.it/xtal_chem_group/index.php,
that builds upon a modernization of codes developed in the last twenty years to introduce frontier methods that focus on the crystalline state of organic compounds and its liquid or solution precursors. The Appendix has a short description of its main features and some flow diagrams are given in ESI.

The CLP and MI-LJC schemes for intermolecular potentials

The establishment of a reliable and affordable scheme for the calculation of intermolecular potentials is upstream of all molecular simulation efforts. In the "classical mechanics" application of Monte Carlo (MC) and Molecular Dynamics (MD) simulation the force field includes an intramolecular part, in terms of harmonic bond stretching and bending potentials, plus torsional functions that describe the restraint to rotations around single bonds. Their parameterization has a long history and will not be discussed here. The intermolecular part is obviously crucial for the reproduction and prediction of the properties of condensed states and can only be of the atom-atom type for affordable MC or **classical** MD calculations. The total energy is a summation of terms in various inverse powers of interatomic distance, driven by a set of parametric coefficients.

The MiCMoS environment offers two choices, both explicitly optimized for organic materials. In the CLP (Coulomb-London-Pauli) scheme[16] the coefficients are derived from combinations of atomic properties like point charge, polarizability and electronegativity; there are no fixed values for given atomic species, but potentials are adapted for each pair of atoms in each new molecule. The whole algebra is embedded in preliminary modules, so that a user need only "push the button" to start a new simulation in a matter of seconds. The MI-LJC (Milano Lennard-Jones-Coulomb) scheme[17] has been calibrated using 377 crystal structures matched to the experimental sublimation enthalpies; it uses usual *R*-6 and *R*-12 Lennard-Jones dispersion-repulsion terms, with transferable parameters for each atomic species. The coefficients of LJ functions are in a library for organic compounds, while atomic point charges for Coulombic potential terms must be obtained from a fitting of the molecular electrostatic potential[25,26] from a high quality

wavefunction. The necessary MO calculation may be expensive for large molecules, but the time investment is needed only once for each molecule. MI-LJC is more accurate for polar or strongly hydrogen-bonded systems, but CLP is more immediate and can be used for preliminaries or to prepare starting computational states for the more accurate treatment. Both schemes are fully transferable, and the user need not roam the literature or an internet browser in search of numbers. However, the functional form of MI-LJC allows user defined parameterization if absolutely necessary.

Monte Carlo (MC) and Molecular Dynamics (MD) in a nutshell

MC is a recursive procedure that changes at random the values of molecular parameters and calculates the new total configurational energy. The change is accepted if $\Delta E < 0$ or, when $\Delta E > 0$, only if $\exp(-\Delta E/RT) > r$, where r is a random number between 0 and 1. T is a formal and invariable temperature parameter. In 10^6-10^7 steps, the procedure "homogenizes" the state, like when a cup of coffee is stirred. Setting a very small T (say 10 K) is equivalent to forced energy decrease and sets MC into an excellent energy-optimization tool. In principle an N-atom molecule can have $3N$-6 degrees of freedom (dof) to be varied; the MiCMoS platform is peculiar in that it allows parts of the molecule to be kept rigid (for a typical example, benzene rings) while torsional variability is allowed over chosen linkages. This is a huge saving in computing resources, because for example toluene is a 7-dof molecule, with three position parameters for the center of mass and three Euler orientation angles plus one torsion dof over the methyl group, and one does not waste time in varying 39 dof's most of which are irrelevant. A MiCMoS user that takes all the defaults on a fully rigid molecule may be ready to run an MC simulation in a few minutes.

Understanding the basics of classical mechanics MD simulation is easy, when its presentation is not obfuscated by mathematical formalism. Consider a single atom oscillating under the influence of a typical intermolecular potential (Figure 2). The system is like a pendulum, except for the strong anharmonicity. If the atom is placed on the right side of the minimum at a certain distance from its attractor, it stabilizes by sliding into the minimum, then uses the acquired velocity to climb a little up the repulsive branch where it is subject to a strong repulsive force. The frames in Figure 2 show the evolution of all the key quantities along the trajectory, being self-explanatory to anyone with an even modest training in physics.

The mathematics under all this is simple: given the potential, the force is calculated as its first derivative, then Newton's equation F = M a is solved to obtain an acceleration, and then the complete velocity/position/energy/force trajectory comes out recursively by numerical (discrete) integration with a finite time step Δt of the order of 1-2 fs (femtoseconds), that scales with the fastest bond dynamics. Of course, a real MD simulation must take into account thousands (nowadays perhaps even millions) of atoms in a model of a crystal or of a liquid, and potentials and forces must be calculated for 10^4-10^6 time steps on all atoms for all intra- and intermolecular dof's. This is orders of magnitude more time-consuming than MC. Using elementary statistical mechanics,[24] temperature is regulated by its equipartition relationship with kinetic energy, and pressure is established via the virial theorem - this at least in simplest applications. The obvious enormous advantage of MD over MC is that the final result of the latter is a static picture of the equilibrium state, while MD gives a "trajectory", that is a picture of the dynamic evolution of the system in time: one knows at each instant where each atom is and what it is doing. MD is to MC like a moving picture is to a photograph.

In a typical application of MiCMoS for the simulation of any condensed system (bulk crystal or liquid, crystal cluster, micelle)

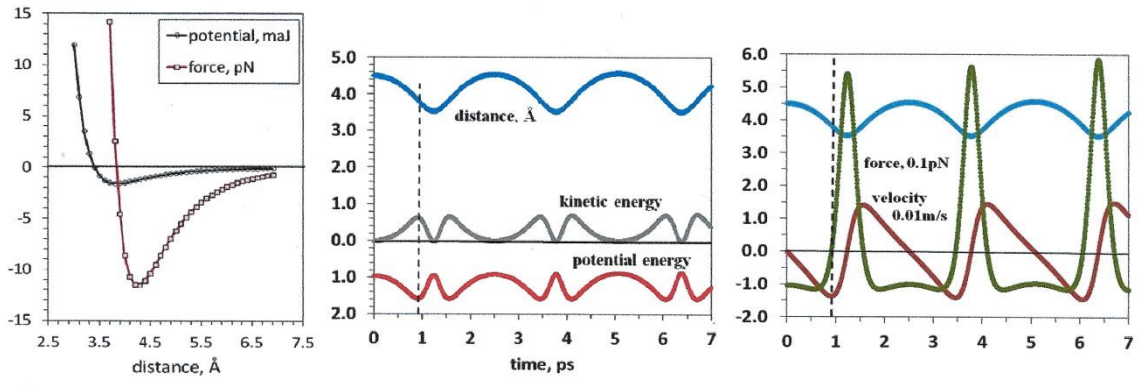

Figure 2. A typical intermolecular potential and force for argon atoms (milliattojoule and piconewton units, maJ and pN). Right frames: The trajectory of an atom under the action of the potential. The vertical dotted line denotes the distance at which the potential energy is minimum.

a molecular model is supplied in the form of Cartesian coordinates or fractional crystal coordinates. There are modules to prepare tentative computational boxes of any size and with any desired degree of order, and to assign force field parameters. An MC preliminary calculation, perhaps in the full default mode, is carried out to dispose of large inhomogeneities and sharp contacts producing a roughly equilibrated computational box ready for a smooth take off of an MD simulation. The platform includes a host of subsidiary modules to analyze single or averaged frames and trajectories to extract physical information from the huge mass of output numbers: total energies to be compared with thermodynamic phase change data; temperature and pressure coefficients (state equations); radial distribution functions for internal structure; diffusion coefficients and rotational correlation times in liquids; bulk moduli and anisotropic compressibility; lattice strain and response to user defined external stress.

Dynamic trajectories can show the atomic level process of intermolecular aggregation, of hydrogen bond formation and breaking, of melting, and, with some luck and ingenuity, can even show a trace of the preliminaries to crystal nucleation. On screen movies generated from coordinate trajectories give an impressive window on the proceedings at atomic level. Most if not all of these features are present also in other platforms, like for example Gromacs,[27] but MiCMoS is the only one explicitly set up for liquid and crystalline states of small molecules rather than oriented to biological macromolecules.

Large-amplitude motions, plastic crystals

Usual crystal packing diagrams show a frozen picture of the structure, misleading in many ways because molecules are always oscillating in thermal libration and quite often also molecular groups or even entire molecules are flipping around even though no trace of these large amplitude motions appears from the X-ray experiment. For example, in our experience with crystal dynamics about 50% of arene methyl groups and a good percent of arene trifluoromethyl groups are freely rotating in the crystal. MD simulations concur with frequent reports of rotationally disordered groups in X-ray work; caution should be used in such cases when defining C-H···X or C-F···X special interactions.[13,28]

As an example of computational detection of such phenomena we present the case of 1,4-cyclohexadiene, whose crystal structure has been determined at 153 K without any report of disorder.[29] The crystal melts at 223 K, a rather high temperature for a C_6 hydrocarbon (n-hexane melts at 177 K) but similar to that of other cyclic compounds, cyclohexane (280 K) and benzene (279 K). The reason is not high cohesive energies, but low melting entropies, because globular molecules are reorienting as a whole in the crystal (recall that $T_{Melting} = \Delta H_M/\Delta S_M$). In fact, an MD simulation of the crystal at 300 K,[30] a temperature set somewhat higher than the melting point to speed up things a little, shows a quick loss of rotational correlation, although the distribution of centers of

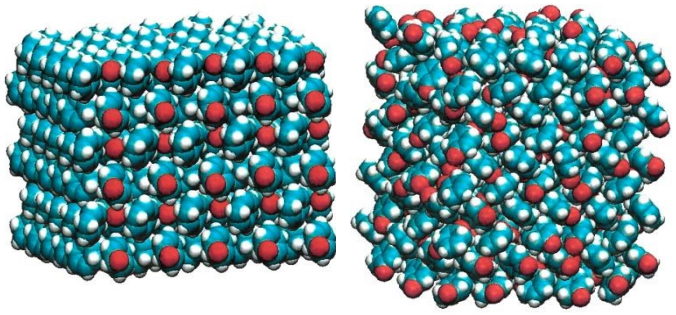

Figure 3. The final frames of 1,4-cyclohexadiene at 153 K (left) and at 300 K (right), with permanence of center of mass positions but loss of orientational correlation. One hydrogen atom has been coloured in red to highlight molecular orientation.

mass remains unaltered (Figure 3). Molecules are spinning around an axis perpendicular to the average molecular plane in what is sometimes called a plastic crystal, that is, a fixed lattice of weakly bound molecules, which are orientationally disorderd.[31] Molecular Dynamics takes care automatically of the necessary cell expansions.

In a properly functionalized material, such a sudden loss of orientational order could be exploited to prepare some sort of solid-state device. In fact, plastic crystals can be considered as the three-dimensional counterpart of liquid crystals.[31] They arise an increasing interest for cutting-edge applications that span from electronic coloured inks[32] to efficient cooling devices based on colossal barocaloric properties.[33] The atomistic picture provided by MD simulations may help describing the subtle time- and temperature-dependent interplay of order-disorder effects by explicitly modelling events that are hardly disentangled experimentally: the possible role of defects, the diffusion kinetics, and the reorientation propensity of a molecule as a function of the chemical nature of its substituents.

Crystal symmetry, real or imaginary

Experimental crystal structures are often analysed in terms of the number and frequency of short intermolecular contacts,[13] to which one is tempted to attribute structural meaning. To go a step further, several force field algorithms exist,[9] also available in mainstream programs,[34] to evaluate intermolecular interaction energies of in-crystal molecular pairs. In the assumption that potential energy contributions are pairwise additive, these energies are useful to recognize what pairs and what symmetries provide a significant part of the total cohesive energy.

On the other hand, it is usually assumed that the X-ray diffraction experiment reveals the actual position and orientation of every molecule in the unit cell, although this assumption is not as obvious as it sounds. X-ray "ordered"

View Article Online
DOI: 10.1039/D1CE01360B

structures may hide frustrated motifs[35] or, even worse, an apparent perfect symmetry could appear when different regions of the bulk crystal are collapsed into unique positions

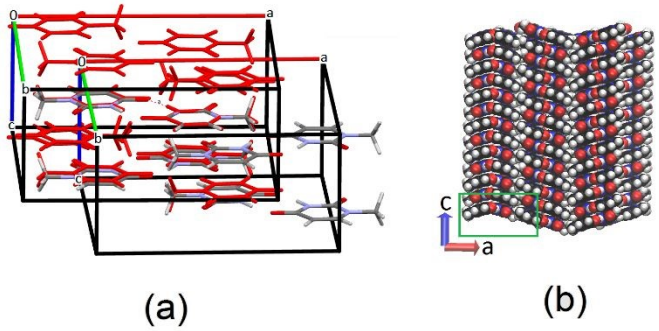

Figure 4. (a) Superimposition of the experimental crystal packing of 1-methyluracil at T = 23 K with the spacetime averaged structure (red molecules) from the last 300 ps of a 400 ps *NpT* MD trajectory (2 fs timestep, LJC force field).[36] The RMSD is 0.0214 Å. (b) Simulation box of 1-methyluracil (3x3x7 unit cells) seen down the *a* axis, time-averaged over the last 300 ps of the trajectory, with one crystallographic cell highlighted.

in the largely time- and space-averaged framework of a structure determination. by X-ray diffraction.

A case in point is that of high resolution ($(\sin\theta/\lambda)_{max}$=1.143 Å^{-1}) X-ray datasets of 1-methyluracil[36] single crystals at 23 K. Difference Fourier maps show two positive peaks (~0.4 e·Å^{-3}) at the molecular extremities, which survive the introduction of high-order aspherical charge density poles and of anharmonic thermal motion; such features appear for all the examined crystals at any resolution level, being therefore related to an intrinsic property of the material.

A possible explanation resides in long-range dynamic disorder, elusive for standard single-crystal methods but within reach of accurate MD simulations. 1-methyluracil crystallizes in the rather unusual I*bam* space group. The asymmetric unit sits on the mirror (*a*,*b*) plane and all atoms but one methyl hydrogen have ½ occupancy factor. The packing consists of perfectly planar parallel sheets, piled up along *c* (Figure 4a). Within each sheet, molecules form planar dimers connected by NH···O hydrogen bonds. When the actual dynamics is explicitly considered in an MD simulation, the structure is no longer planar (Figure 4b). A commensurate stationary modulation with λ ~ 25 Å appears along the *a* axis, resulting in a slanted column motif that maximizes the intermolecular dispersive interactions.[37] When the simulation box is spatially averaged into the standard cell settings, out-of-phase oscillations from different regions cancel out and the experimental X-ray structure is recovered (Figure 4a).

MD simulations indicate that the perfect mirror symmetry in the (*a*,*b*) plane is only a spacetime average. The take home lesson here is that appearing structural properties are sometimes intertwined with hidden dynamics, overlooked when only the static, average X-ray structure is considered. X-ray diffraction does not always have the last word: the consequences of missed dynamics on materials properties are obvious!

Survival times of crystalline clusters

It is perhaps self evident and anyway commonly accepted that early embryos in the process of crystallization from liquid or from solution must be small aggregates of variable size **but** unspecified structure. Are these embryos liquid-like or crystalline? Probing directly the aggregation from a disperse system is too time consuming (order of magnitude of micro- to milliseconds) to be accessible to an MD simulation. The complete transformation of a liquid into its crystal, the Holy Grail of molecular simulation, is out of reach for technical reasons, because the time span is too large, and for physical reasons, because it is extremely difficult to account for the joint effects of temperature, pressure, concentration and a host of other boundary conditions. More viable is a simulation of the inverse process, observing the dynamics of a small crystalline aggregate in a neat computer experiment asking the fundamental question: what is the lifetime of a crystalline cluster, either isolated or solvated?

When running simulations without periodic boundary conditions, isolated clusters may become prone to center-of-mass drift and may develop a net overall rotational momentum. Moreover, border molecules may evaporate away. All these events are undesirable for their adverse consequences on the continuity of trajectories and on the calculation of correlation functions. A unique feature of the MiCMoS MD modules is an astute coding of regressive algorithms[38] to dispose of all these nuisances.

The molecule for our case study is succinic anhydride. Crystalline parallelepiped slabs are first prepared by three-dimensional expansion of the unit cells from the experimental X–ray structure.[39] By trimming out corner molecules, globular nanocrystals are then obtained with 49, 105 and 273 molecules. The 105-molecule cluster is immersed in a well equilibrated 1458–molecule, cubic solvent box (chloroform or methanol): merging programs replace solvent molecules with solute molecules at the core of the liquid box, at the same time deleting corner solvent molecules.

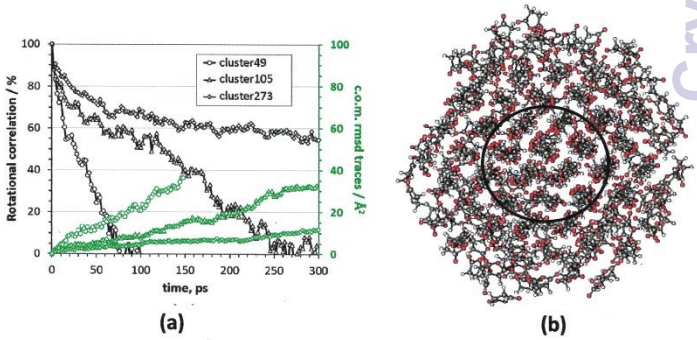

Figure 5. (a) MD results for clusters of succinic anhydride of various size. Rotational correlation functions (black, left ordinate) and diffusion

traces (green, right ordinate) clearly show the effect of cluster size. (b) 273–molecules cluster at 200 ps, showing persistence of a semi–crystalline nucleus (black circle).

Successive MC runs in which solute molecules are not allowed to move from the crystal structure relax the solvation sphere to yield a perfectly crystalline core of solutes surrounded by a globular cloud of solvents, ready to be input to an MD simulation. All coordinate manipulations are comfortably carried out using MiCMoS auxiliary modules. Room temperature MD runs are then carried out on the naked or solvated aggregates for a time long enough to observe any occurring structural evolution. For a comparison of radial distributions and correlation functions, also bulk crystals and bulk liquids were simulated by MC.

As expected, a marked size effect appears (Figure 5a). Smaller clusters collapse to a liquid in less than half nanosecond, and only the largest cluster seems to survive a bit longer, as a crystal–like core remains embedded in a liquid surface layer. The hint from this simulation is **that** liquefaction proceeds from the surface to the core as implied by surface–melting theories.

Figure 6 shows the effects of solvation. Persistence of the crystalline structure increases on going from the bare cluster to the chloroform solvate to the methanol solvate, in correlation with the increasing strength of intermolecular interactions from vacuum to solvents of increasing polarity. Nevertheless, the fate of the embedded cluster is anyway an evolution to a liquid structure, as shown pictorially in Figure 7.

What is one to make of these results? On the technical side, note that a special feature of the MiCMoS post-analysis programs allows a normalization of the RDF's also for small aggregates, and that the smooth behavior of the correlation functions confirms that the algorithm for quenching overall rotational and translational momenta is effective.

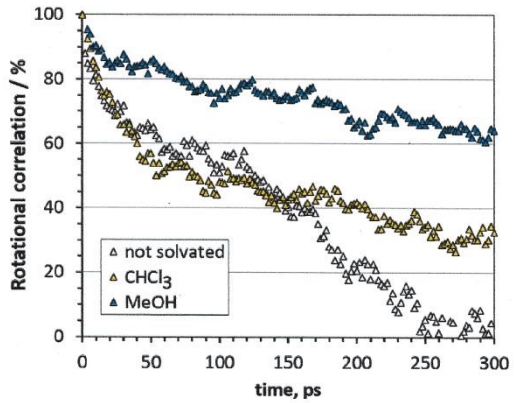

Figure 6. Rotational correlation traces for MD runs on a solvated 105-molecule cluster of succinic anhydride. Evolution to a liquid structure is fastest in the bare cluster, and faster in chloroform than in methanol.

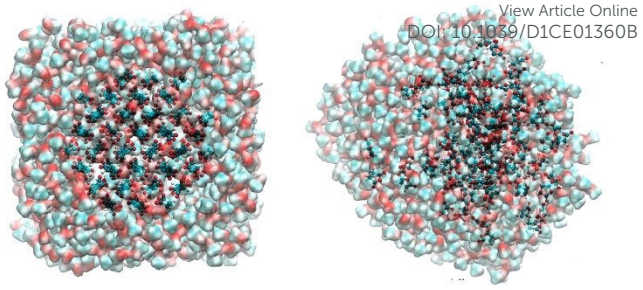

Figure 7. Pictorial views of solvated 105–molecules clusters of succinic anhydride: starting (a) and final (after 1000 ps) (b) states of the MD run in methanol.

As for the physics, MD is a simulation, not reality, and can only give hints at what might happen. In this case the hints are persistent against changes in cluster size and shape, in chemical nature and simulation conditions: nanocrystals of up to 200 molecules invariably relax immediately to a partly or totally liquid–like structure. The downstream suggestion is that early aggregation species cannot be immediately crystalline, as often postulated by classical nucleation theory (CNT), and most likely must go through amorphous states, in a perfect picture of postulated two-step nucleation mechanisms.[40] A highly promising lead for future research is the investigation of the effects of chemical potentials on growing nuclei by introduction of a shell of free solute molecules in the solvent layer around the central nucleus.

Anisotropic response to external pressure

The development of efficient diamond anvil cells (DACs) in the 1970s paved the way to high-pressure crystallography (HPC).[41] Nowadays, HPC is employed in conjunction with synchrotron sources and advanced spectroscopic techniques[42] to explore the behaviour of crystalline materials at extreme conditions. These studies are important in many fields of practical application: for example, active pharmaceutical ingredients may undergo phase changes when compressed by a few GPa by grinding in a mortar,[43] or during tablet preparation.

High pressure may change materials response in many other ways: typically, absorption and luminescence properties of crystalline polyacenes[44] are strongly pressure-dependent, because the angle between aromatic cores and thus the degree of π···π overlap are sensitive to the applied external stress. Anthracene is a prototypical molecular material for electro-optic devices. It crystallizes in the centrosymmetric $P2_1/a$ space group by adopting a classical herringbone motif. Its high-pressure behaviour was probed by X-ray powder diffraction up to 10 GPa.[45] However, conflicting evidences exist on the occurrence of high-*P* structural transformations. A phase transition was reported between 1 and 3 GPa,[46] but other studies[45,47] could not reproduce these results. Later, the

View Article Online
DOI: 10.1039/D1CE01360B

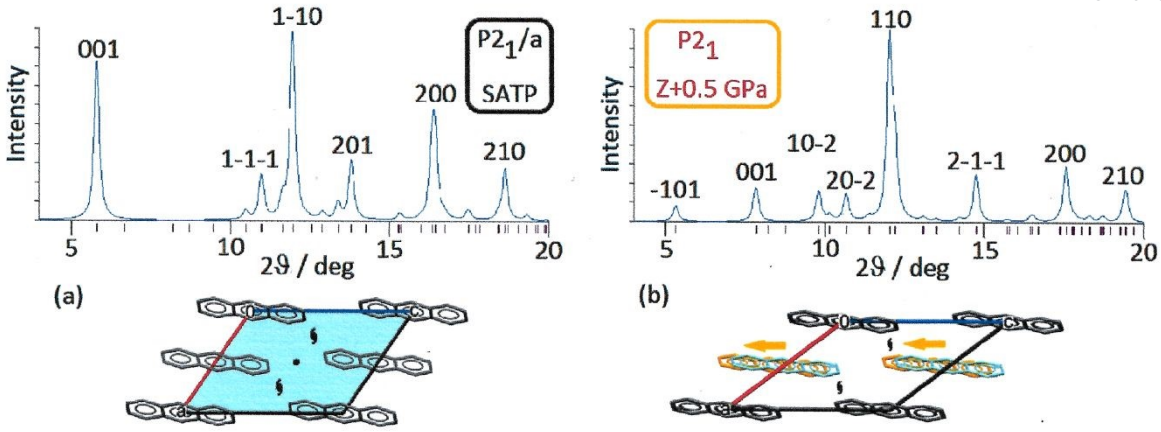

Figure 8. First row: simulated powder pattern for the spacetime average structure of anthracene under isotropic compression of 1 bar (a) and after applying an anisotropic compression of +0.5 GPa roughly along *c* (b). The patterns correspond to the experimental wavelength of 0.9204 Å and the hkl indices of the main reflections are shown. Second row: crystal packing corresponding to the above powder patterns, seen along *b* and with symmetry elements highlighted (cyan: glide planes; black: screw axes). In the $P2_1$ structure on the right, alternate rows of molecules at ½ *a* (yellow) slip along the direction indicated by the arrow and destroy the original *a* symmetry (marked by cyan molecules).

occurrence of a reversible phase transition in the 10-15 GPa range was confirmed by the appearance of new (unindexed) Bragg peaks in the powder diffraction pattern, although these reflections were too few to permit a structure determination.[48] As the onset of the transition was strongly medium-dependent, it was concluded that this high-*P* behaviour is likely to be due to imperfect control of hydrostatic conditions.[48]

MD simulations of the anthracene crystal structure subject to input mechanical stress are ideal to investigate this matter, because they provide a molecular level picture of any process occurring in the crystal, which can be easily compared with experimental X-ray results. In agreement with previous findings, the $P2_1/a$ symmetry of anthracene is conserved up to 30 GPa if the applied stress is perfectly hydrostatic. On the contrary, even a moderate anisotropic compression invariably implies some reduction of symmetry, with a significant influence on the equilibrium structure. A 0.5 GPa excess compression along the *Z* laboratory axis, roughly coincident with the *c* edge, does not greatly alter the centre of mass distances in the first molecular coordination shell but causes the monoclinic angle to increase by ≈12 deg, and eventually breaks the glide symmetry in the (*a*,*b*) plane (Figure 8). Accordingly, a low-angle (-101) reflection appears, which is forbidden in $P2_1/a$ but is compatible with the experimental X- ray powder pattern found above 10 GPa.[48] Symmetry checks[49] quantify the symmetry reduction by suggesting a $P2_1$ space group for high-*P* phase. If confirmed, the existence of polar structures at high pressure for polyacenes might lead to novel electro-optical applications, including the design of accurate pressure sensors.

Summary and final remarks

Our effort in this Highlight has been firstly dedicated to recollection of a bit of history, to the illustration of a few basic concepts in molecular simulation, and to a brief review of theoretical intermolecular potential formulations explicitly derived for the treatment of non polymeric organic molecules. Modeling organic materials consisting of entities in the 100-1000 dalton range requires capabilities for structure retrieval from databases, for molecular structure generation and handling, for assignment of intra- and intermolecular potentials, and for the construction of computational boxes of any desired degree of ordering, from pure isotropic liquids to solution to partially ordered systems to crystalline substrates. Downstream of the two typical tools of the simulation trade, Monte Carlo and Molecular Dynamics, a number of modules are necessary to extract chemical information from the resulting trajectories, making sense of long lists of numbers. The advantages of having all software encompassed in a single platform are too many to be listed, the main one being perhaps the total and seamless intercommunication between processing modules, upstream and downstream. This is what has been hopefully accomplished in our newly developed MiCMoS computer program package for "small" molecules.

The rest of the Highlight, as might have been expected, provides a few examples of what can nowadays be done: molecular rearrangements and plastic crystals; detection of supersymmetries; evolution of crystalline clusters, naked and solvated; interpretation of problematic pressure-dependent experimental data, all easily handled in the MiCMos environment without recourse to transcendental computer resources. Its ambition is to emerge from the deep sea of pure theoretical chemistry to offer help and illumination also to the practicing solid state chemist with limited experience in computing.

Appendix: detail of the MiCMoS platform

The MiCMoS platform is a set of separate Fortran programs (modules), accessible through registration and downloading (https://sites.unimi.it/xtal_chem_group/index.php/research/5-micmos), with open source codes that the user can peruse and modify. There are no fees and no restrictions on accessibility, except for the obvious ones related to fair use. The code in the platform is divided in two sections. Section A has modules that perform data retrieval from CSD Databases or user *cif* files, renormalization of hydrogen atoms, calculation of point charges for the AA-CLP potential scheme, and atom-atom lattice energy and crystal packing analysis; also included are modules for preparation of data and execution of PIXEL lattice energy calculations. Section B has modules for Monte Carlo and Molecular Dynamics simulation, with a set of about 20 separate auxiliary modules that carry out the preparation of crystal and liquid computational boxes, solution boxes, and other kinds of binary systems; preparation of the topology files with library force field parameters for common organic molecules; trajectory analyses and radial distribution function calculations, and other kinds of geometrical checks on MC or MD results. The standard topology files can be altered by inclusion of force field parameters from other schemes (AMBER, GROMACS, CHARMm) within the limitations of the embedded force field functional forms, that can however be modified locally by users with a modest knowledge of Fortran programming. Intermolecular energies can also be computed by the more refined MI-LJC potential scheme that requires high level (ideally, MP2/6-31G**) ESP-derived point charges; any other 6-12-*q* parameters can be applied optionally. The MD modules include a special feature for the quenching of translational and rotational momenta in non-periodic simulations.

In practice, the user should download the source codes, compile them, and execute each module on in-house machines either in MS-DOS or Unix environments, since all executions proceed from line I/O files and batch commands. A large number of test input and output data are supplied, also organized in detailed tutorials (https://sites.unimi.it/xtal_chem_group/index.php/tutorials). The Supplementary Information has flowcharts for the module sequences in the two Sections.

Electronic Supplementary Information

Flowcharts of the organization of the MiCMoS modules (file flowchart.docx).

Author Contributions

A. Gavezzotti provided the main framework, the introductory sections and part of the results. L. Lo Presti contributed sections on hidden symmetry and pressure control. L. Lo Presti and S. Rizzato are jointly in charge of the maintenance of the MiCMoS platform and were in charge of its description, of literature surveys and of the final layout of the paper.

Conflicts of interest

There are no conflicts to declare.

Notes and references

View Article Online
DOI: 10.1039/D1CE01360B

1 H. Winick, in *Proceedings of the 1997 Particle Accelerator Conference (Cat. No.97CH36167)*, IEEE, 2001, vol. 1, pp. 37–41.

2 M. Levantino, B. A. Yorke, D. C. F. Monteiro, M. Cammarata and A. R. Pearson, *Curr. Opin. Struct. Biol.*, 2015, **35**, 41–48.

3 K. Nass, A. Gorel, M. M. Abdullah, A. V. Martin, M. Kloos, A. Marinelli, A. Aquila, T. R. M. Barends, F. J. Decker, R. Bruce Doak, L. Foucar, E. Hartmann, M. Hilpert, M. S. Hunter, Z. Jurek, J. E. Koglin, A. Kozlov, A. A. Lutman, G. N. Kovacs, C. M. Roome, R. L. Shoeman, R. Santra, H. M. Quiney, B. Ziaja, S. Boutet and I. Schlichting, *Nat. Commun.*, 2020, **11**, 1–9.

4 S. M. Bak, Z. Shadike, R. Lin, X. Yu and X. Q. Yang, *NPG Asia Mater.*, 2018, 10, 563–580.

5 H. Zettergren, A. Domaracka, T. Schlathölter, P. Bolognesi, S. Díaz-Tendero, M. Łabuda, S. Tosic, S. Maclot, P. Johnsson, A. Steber, D. Tikhonov, M. C. Castrovilli, L. Avaldi, S. Bari, A. R. Milosavljević, A. Palacios, S. Faraji, D. G. Piekarski, P. Rousseau, D. Ascenzi, C. Romanzin, E. Erdmann, M. Alcamí, J. Kopyra, P. Limão-Vieira, J. Kočišek, J. Fedor, S. Albertini, M. Gatchell, H. Cederquist, H. T. Schmidt, E. Gruber, L. H. Andersen, O. Heber, Y. Toker, K. Hansen, J. A. Noble, C. Jouvet, C. Kjær, S. B. Nielsen, E. Carrascosa, J. Bull, A. Candian and A. Petrignani, *Eur. Phys. J. D*, 2021, **75**, 152.

6 T. Nakane, A. Kotecha, A. Sente, G. McMullan, S. Masiulis, P. M. G. E. Brown, I. T. Grigoras, L. Malinauskaite, T. Malinauskas, J. Miehling, T. Uchański, L. Yu, D. Karia, E. V. Pechnikova, E. de Jong, J. Keizer, M. Bischoff, J. McCormack, P. Tiemeijer, S. W. Hardwick, D. Y. Chirgadze, G. Murshudov, A. R. Aricescu and S. H. W. Scheres, *Nature*, 2020, **587**, 152–156.

7 C. R. Groom and F. H. Allen, *Angew. Chemie Int. Ed.*, 2014, **53**, 662–671.

8 A. Gavezzotti, *The Crystalline States of Organic Compounds, Volume 20*, Elsevier, 1st edn., 2021.

9 A. Gavezzotti and L. Lo Presti, *Cryst. Growth Des.*, 2015, **15**, 3792–3803.

10 A. Gavezzotti and L. Lo Presti, *Cryst. Growth Des.*, 2016, **16**, 2952–2962.

11 A. Gavezzotti, S. Rizzato and L. Lo Presti, *Cryst. Growth Des.*, 2018, **18**, 7219–7227.

12 A. Gavezzotti and S. Rizzato, *J. Org. Chem.*, 2014, **79**, 4809–4816.

13 L. Lo Presti, *CrystEngComm*, 2018, **20**, 5976–5989.

14 G. Filippini and A. Gavezzotti, *Acta Crystallogr. Sect. B Struct. Sci.*, 1993, **49**, 868–880.

15 A. Gavezzotti, *CrystEngComm*, 2003, **5**, 429–438.

16 A. Gavezzotti, *New J. Chem.*, 2011, **35**, 1360–1368.

17 A. Gavezzotti, L. Lo Presti and S. Rizzato, *CrystEngComm*, 2020, **22**, 7350–7360.

18 J. S. Chickos and A. Gavezzotti, *Cryst. Growth Des.*, 2019, **19**, 6566–6576.

19 R. Dovesi, A. Erba, R. Orlando, C. M. Zicovich-Wilson, B. Civalleri, L. Maschio, M. Rérat, S. Casassa, J. Baima, S. Salustro and B. Kirtman, *Wiley Interdiscip. Rev. Comput. Mol. Sci.*, 2018, **8**, 1360.
20 C. Sutton, M. S. Marshall, C. D. Sherrill, C. Risko and J. L. Brédas, *J. Am. Chem. Soc.*, 2015, **137**, 8775–8782.
21 J. Moellmann and S. Grimme, *J. Phys. Chem. C*, 2014, **118**, 7615–7621.
22 W. L. Jorgensen and C. J. Swenson, *J. Am. Chem. Soc.*, 1985, **107**, 569–578.
23 R. Car and M. Parrinello, *Phys. Rev. Lett.*, 1985, **55**, 2471–2474.
24 W. F. van Gunsteren and H. J. C. Berendsen, *Angew. Chemie Int. Ed. English*, 1990, 29, 992–1023.
25 U. C. Singh and P. A. Kollman, *J. Comput. Chem.*, 1984, **5**, 129–145.
26 B. H. Besler, K. M. Merz and P. A. Kollman, *J. Comput. Chem.*, 1990, **11**, 431–439.
27 M. J. Abraham, T. Murtola, R. Schulz, S. Páll, J. C. Smith, B. Hess and E. Lindah, *SoftwareX*, 2015, **1–2**, 19–25.
28 R. Taylor, *Cryst. Growth Des.*, 2016, 16, 4165–4168.
29 G. A. Jeffrey, J. Buschmann, C. W. Lehmann and P. Luger, *J. Am. Chem. Soc.*, 1988, **110**, 7218–7219.
30 A. Gavezzotti and L. Lo Presti, *J. Appl. Crystallogr.*, 2019, **52**, 1253–1263.
31 R. M. Pick, in *Liquid Crystals of One- and Two-Dimensional Order, Springer Series in Chemical Physics, vol 11*, eds. W. Helfrich and G. Heppke, Springer, Berlin, Heidelberg, 1980, pp. 47–48.
32 B. Liu, T. H. Besseling, M. Hermes, A. F. Demirörs, A. Imhof and A. Van Blaaderen, *Nat. Commun.*, 2014, **5**, 1–8.
33 P. Lloveras, A. Aznar, M. Barrio, P. Negrier, C. Popescu, A. Planes, L. Mañosa, E. Stern-Taulats, A. Avramenko, N. D. Mathur, X. Moya and J. L. Tamarit, *Nat. Commun.*, 2019, **10**, 1–7.
34 C. F. Macrae, I. Sovago, S. J. Cottrell, P. T. A. Galek, P. McCabe, E. Pidcock, M. Platings, G. P. Shields, J. S. Stevens, M. Towler and P. A. Wood, *J. Appl. Crystallogr.*, 2020, **53**, 226–235.
35 G. Macetti, L. Loconte, S. Rizzato, C. Gatti and L. Lo Presti, *Cryst. Growth Des.*, 2016, **16**, 6043–6054.
36 R. Destro, P. Roversi, M. Barzaghi and L. Lo Presti, *Molecules*, 2021, **26**, 3075.
37 V. Colombo, L. Lo Presti and A. Gavezzotti, *CrystEngComm*, 2017, **19**, 2413–2423.
38 A. Gavezzotti and L. Lo Presti, *New J. Chem.*, 2019, **43**, 2077–2084.
39 V. Ferretti, P. Gilli and A. Gavezzotti, *Chem. - A Eur. J.*, 2002, **8**, 1710–1718.
40 D. Erdemir, A. Y. Lee and A. S. Myerson, *Acc. Chem. Res.*, 2009, **42**, 621–629.
41 A. Katrusiak, *Acta Crystallogr. A.*, 2008, **64**, 135–48.
42 M. Guerain, *J. Pharm. Sci.*, 2020, 109, 2640–2653.
43 C. Lefebvre, A. M. Guyot-Hermann, M. Draguet-Brughmans, R. Bouché and J. C. Guyot, *Drug Dev. Ind. Pharm.*, 1986, **12**, 1913–1927.
44 G. Horowitz, *Adv. Mater.*, 1998, **10**, 365–377.
45 M. Oehzelt, R. Resel and A. Nakayama, *Phys. Rev. B*, 2002, **66**, 174104.
46 L. Zhao, B. J. Baer and E. L. Chronister, *J. Phys. Chem. A*, 1999, **103**, 1728–1733.
47 R. Pufall and J. Kalus, *Acta Crystallogr. Sect. A*, 1988, **44**, 1059–1065.
48 R. Resel, M. Oehzelt, K. Shimizu, A. Nakayama and K. Takemura, *Solid State Commun.*, 2004, **129**, 103–106.
49 A. L. Spek, *Acta Crystallogr. Sect. D Biol. Crystallogr.*, 2009, **65**, 148–155.

View Article Online
DOI: 10.1039/D1CE01360B